Contemporary Engineering Sciences, Vol. 10, 2017, no. 32, 1551 - 1559
HIKARI Ltd, www.m-hikari.com
https://doi.org/10.12988/ces.2017.711181

Fractal Design Approach for Heat Sinks Using L-Systems

Fernando Martínez Santa

Universidad Distrital Francisco José de Caldas
Bogotá, Colombia

Holman Montiel Ariza

Universidad Distrital Francisco José de Caldas
Bogotá, Colombia

Fredy Martínez Sarmiento

Universidad Distrital Francisco José de Caldas
Bogotá, Colombia

Copyright © 2017 Fernando Martínez Santa, Holman Montiel Ariza and Fredy Martínez Sarmiento. This article is distributed under the Creative Commons Attribution License, which permits unrestricted use, distribution, and reproduction in any medium, provided the original work is properly cited.

Abstract

This paper shows the results of modeling fractal heat sink structures by means of using a formal grammar implementing an L-System. This approach uses a simple L-System with 3 variables and 3 replacement rules, restricting the rotation angle to 90°. A total of 10 heat sink structures were modeled with this method, after that, they were simulated the Finite Element Method (FEM) in order to do temperature measurements and determine their performance. Those simulations used aluminum as material and temperatures from 20 to 100° Celsius. As a result, 6 of the 10 proposed structures showed improvements compared to a reference regular heat sink structure that was modeled as an L-System too. According to a proposed performance index based on the average temperature and the used area of the modeled structure, improvements from 6 to 31% were reached.

Keywords: Heat sink, Fractal design, L-system, Thermal FEM

1 Introduction

Almost since the creation of the fractal theory, the different kinds of fractals have been used in a lot of different applications. Specifically, in engineering there are a huge amount of implementations, for instance in antenna design, inspired on Sierpinsky carpet and triangle [1] and Peano fractal [2], and other ones [3]–[8]. Also, fractals have been used in filter design, especially for wireless communications [9]–[11] and for stretchable electronics [12]. In the area of heat transfer and conduction, the fractal design has been evaluated too [13], [14].
On the other hand, L-Systems or Lindenmayer systems are one way to represent fractal or self-similar structures, and they are very used due to their simple implementation. L-Systems consist of a drawing system based on a formal grammar and an iterative replacement structure. These system have been used mainly in biology for modeling the plants growing [15]–[17], but there are several applications on engineering for designing structures [18]–[21], in areas as diverse as robotics, computer graphics and heat conduction. The main purpose of this work, is to keep exploring the use of L-Systems as design approach for heat sinks, taking advantage of their iterative structure to obtain relative complex structures.

2 Methodology

A simple L-System was implemented to represent several heat sink structures, which were designed taking as principle, the maximization of the area in contact to air. It was a 2D L-System, that means it was possible to represent only a profile or axial cut of the final 3D structure, in order to simplify the design and the later simulation. After obtaining the 2D heat sink shapes from L-System, they were simulated using the Finite Element Method (FEM) by means of using Matlab® PDE toolbox (Partial Differential Equations), over the same temperature conditions, in order to obtain thermal average measurements to compare the different resultant structures. A total of 11 simulations were done, a reference regular heat sink structure (modeled as an L-System too) and other 10 fractal structures.

2.1 L-System

For all the designed structures, for the L-System, a Θ rotation angle was fixed 90°, in order to obtain only straight-angle shapes, starting from an initial angle of 0° and adding Θ when a "+" appears or subtracting Θ when "-". The used L-System use a total of three variables (*F*, *G* and *H*) and three replacement rules. The number of iterations changed between 2 and 4. For instance a regular heat sink structure (in this case a comb-shaped heat sink with 16 teeth), as the one shown in Figure 1a, can be described as follows:

variables:	$F\ G\ H$
axiom:	$-G+F+G-$
rules:	$(F \rightarrow F+G-H-G+F)\ (G \rightarrow G)\ (H \rightarrow H)$

rotation angle Θ: *90°*
drawing length: *F(1) G(16) H(1)*
iterations: *4*

And the first fractal design (shown in Figure 1b) was described as follows:

variables: *F G H*
axiom: *F*
rules: *(F → G+F-H-F+G) (G → GG) (H → G-F+H+F-G)*
rotation angle Θ: *90°*
drawing length: *F(1) G(1) H(1)*
iterations: *4*

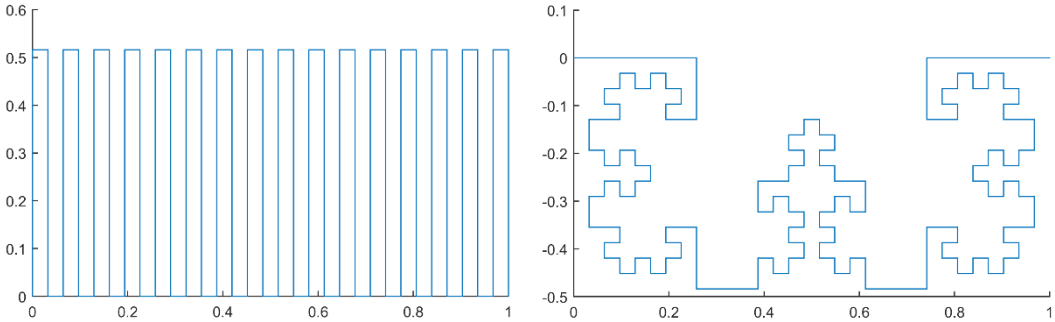

Figure 1: Structures obtained by using the L-System: a) regular head sink, b) a fractal one.

Additionally, the designed L-System normalizes the obtained structures in the *x* axis, in order to make easy the later comparation between all the obtained designs. With the purpose of making feasible a future real manufacturing of the designs, all of them were restricted to have beams (or teeth) from 0.02 to 0.04, then it was necessary to change the number of iterations in each case to adjust the obtained shape to this restriction. Due to the *x* axis was normalized, the design has not dimension units, then the restriction of the beams size has not units neither, but it was based on the tooth size of the reference sink head structure (normalized too) as the one shown in Figure 1a.

2.2 FEM simulations

After obtaining the heat sink structures by means of using the designed L-System, these were completed as a closed polygon without overlapping lines. Then, the polygons were simulated using FEM, where aluminum where chosen as main material. For each FEM simulation a fine meshing was used, producing around 1200 nodes by structure. For all the simulations, a temperature of 100° Celsius was placed in the bottom surface (line) and a 20° Celsius for the rest. The elliptic heat

transfer equation was used with a convective heat transfer coefficient of 1 and a heat conduction coefficient of 205 (aluminum). The results of the simulation of the reference heat sink is shown in the Figure 2, where an average temperature of 27.3° Celsius was obtained.

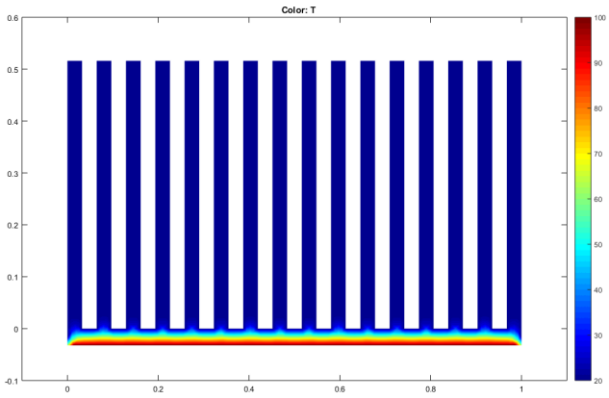

Figure 2: FEM simulation of the reference regular heat sink. Colors indicate the temperature, from 100° (dark red) to 20° (dark blue) Celsius.

3 Results

A total of 11 heat sink structures were modeled using L-Systems, one reference standard heat sink numbered as 1, and other 10 fractal ones numbered from 2 to 11. The axiom, rules and number of iterations of the L-System change depending on the desired shape, Table 1 show these features for all the modeled structures. All the L-Systems that generate fractal heat sink structures (2 to 11) share these features:

variables:	*F G H*
number of rules:	*3*
rotation angle Θ:	*90°*
drawing length:	*F(1) G(1) H(1)*

Additionally, All the generated structures were simulated by means of using FEM, were the average temperature was obtained as well as the used volume of the heat sink (percentage of the surrounding rectangle area in 2D). This last feature is important to optimize the used material in the manufacturing process, also it has a direct relationship with surface area (contour line), that is important to the convective heat transfer to the air. The relationship between the average temperature and the percentage area was taken as performance *P* value applying the equation 1.

Table 1: Axiom, rules and number of iterations of all the structures modeled with L-Systems.

	Axiom	Rule 1	Rule 2	Rule 3	I
1	*-G+F+G-*	*F → F+G-H-G+F*	*G → G*	*H → H*	4
2	*F*	*F → G+F-H-F+G*	*G → GG*	*H → G-F+H+F-G*	4
3	*F*	*F → G-F+H+F-G*	*G → GG*	*H → G+F-H-F+G*	4
4	*F*	*F → F+GG-H-GG+F*	*G → GG*	*H → G-FF+HH+FF-G*	3
5	*F-G-F+G+HHH+G+F-G-F*	*F → F-G+H+G-F*	*G → GGG*	*H → H+GG-F-GG+H*	2
6	*F-H-F+G+HHH+G+F-H-F*	*F → F-G+H+G-F*	*G → GG*	*H → H+G-F-G+H*	2
7	*F-HF+H+FH-F*	*F →F-GG+H+GG-F*	*G → GGG*	*H → H+G-F-G+H*	2
8	*F-HF+HH+FH-F*	*F → F-GG+H+GG-F*	*G → GGG*	*H → H+GG-F-GG+H*	2
9	*F+G+F-G-HHH-G-F+G+F*	*F → F+G-H-G+F*	*G → GGG*	*H → H-GG+F+GG-H*	2
10	*F+HF-H-FH+F*	*F → F+GG-H-GG+F*	*G → GGG*	*H → H-G+F+G-H*	2
11	*F+HF-HH-FH+F*	*F → F+GG-H-GG+F*	*G → GGG*	*H → H-GG+F+GG-H*	2

$$P = \frac{1}{(T_{av} - T_{ext}) * A_p} \quad (1)$$

Where, T_{av} is the average temperature over all the nodes of the FEM simulation., T_{ext} is the reference temperature (20° Celsius) and A_p is the percentage of the used area of the surrounding rectangle of the shape. The results are shown in Table 2, Figure 3 and Figure 4. Table 2 associates the results and the structures shown in Figures 3 and 4.

Table 2. Results of the FEM simulations of the obtained structures.

	Figure	Av. Temp.	% Area	Performance	Improvement
1	2,00	27,33	0,54	0,25	0,00
2	3a	28,13	0,38	0,33	0,31
3	3b	27,47	0,69	0,19	-0,23
4	3c	32,64	0,73	0,11	-0,57
5	3d	26,29	0,64	0,25	-0,01
6	3e	27,94	0,56	0,22	-0,11
7	4a	27,29	0,48	0,29	0,15
8	4b	27,55	0,51	0,26	0,04
9	4c	26,06	0,54	0,31	0,23
10	4d	26,54	0,58	0,27	0,06
11	4e	26,60	0,53	0,29	0,15

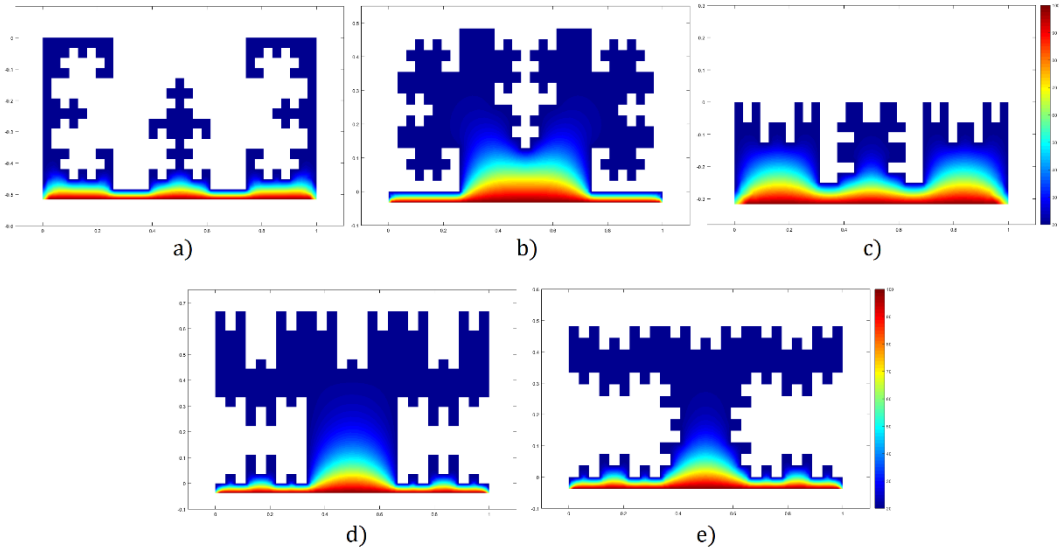

Figure 3: FEM simulation of the structures number 2 to 6.

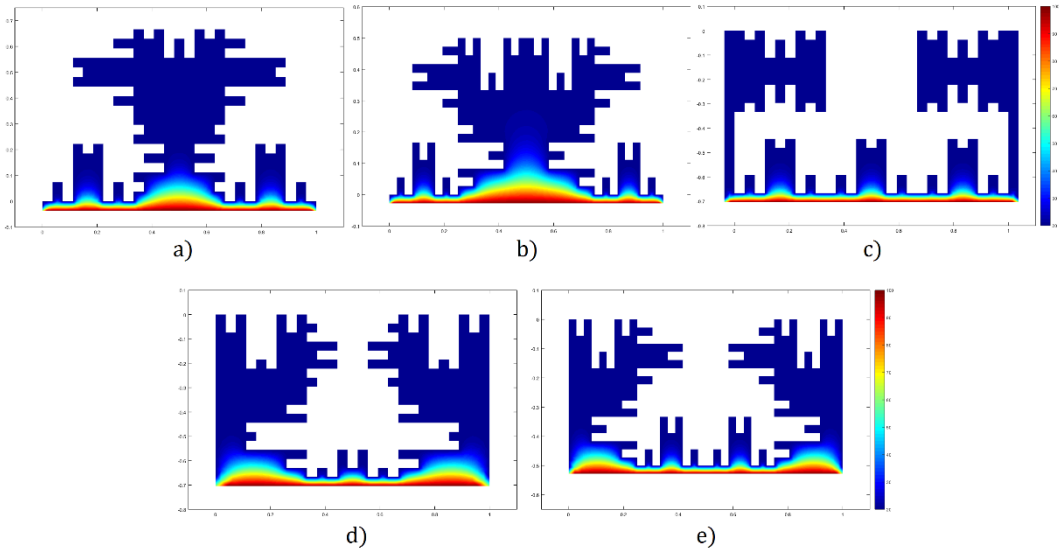

Figure 4: FEM simulation of the structures number 7 to 11.

4 Conclusion

It is totally feasible to model heat sink structures using a formal grammar by means on an L-System as the proposed one, using a limited number of variables and replacement rules. Increasing the number of iterations, it is possible to maximize the border of the resultant shape, increasing at the same time the area in contact with the air, but this increase is limited by manufacturing size restrictions.

As shown in table 2, 4 of the 10 modeled heat sink structures, did not show any improvement than the standard reference, according with que performance index proposed in the equation 1, but the other 6 improved the standard from 6 to 31%.

5 Future work

It is wanted to do several 3D 3FEM simulations that take into account the convective heat transfer between the metallic material and the air, in order to compare and/or validate the results presented in this text.
A possible improvement of this approach is to modify the original resultant fractal structures, turning them into "thinner" ones in order to reduce the amount of material for the manufacturing process and at the same time increase the surface in contact with the air.
Classical fractal curves like Hilbert curve will maximize the area in contact to the air for this kind of application, so it is possible to explore that curves with a limited amount of iterations.

Acknowledgements. The authors thank to the Universidad Distrital Francisco José de Caldas and the ARMOS Research group for supporting this researching.

References

[1] C. de Lucena Nóbrega, M. Ribeiro da Silva, P. H. da Fonseca Silva, and A. G. D'Assunção, A compact frequency selective surface with angular stability based on the Sierpinski fractal geometry, *J. Electromagn. Waves Appl.*, **27** (2013), no. 18, 2308–2316. https://doi.org/10.1080/09205071.2013.842939

[2] H. Oraizi and S. Hedayati, Miniaturized UWB monopole microstrip antenna design by the combination of Giusepe Peano and Sierpinski carpet fractals, *IEEE Antennas Wirel. Propag. Lett.*, **10** (2011), 67–70. https://doi.org/10.1109/lawp.2011.2109030

[3] D. H. Werner and S. Ganguly, An overview of fractal antenna engineering research, *IEEE Antennas Propag. Mag.*, **45** (2003), no. 1, 38–57. https://doi.org/10.1109/map.2003.1189650

[4] F. Viani, M. Salucci, F. Robol, G. Oliveri, and A. Massa, Design of a UHF RFID/GPS fractal antenna for logistics management, *J. Electromagn. Waves Appl.*, **26** (2012), no. 4, 480–492. https://doi.org/10.1163/156939312800030640

[5] L. Lizzi and G. Oliveri, Hybrid design of a fractal-shaped GSM/UMTS antenna, *J. Electromagn. Waves Appl.*, **24** (2010), no. 5–6, 707–719. https://doi.org/10.1163/156939310791036386

[6] S. F. Jilani, H. Ur-Rahman and M. N. Iqbal, Novel star-shaped fractal design of rectangular patch antenna for improved gain and bandwidth, *Antennas and Propagation Society International Symposium (APSURSI) IEEE*, (2013),

1486–1487. https://doi.org/10.1109/aps.2013.6711402

[7] N. Bayatmaku, P. Lotfi, M. Azarmanesh and S. Soltani, Design of simple multiband patch antenna for mobile communication applications using new E-shape fractal, *IEEE Antennas Wirel. Propag. Lett.*, **10** (2011), 873–875. https://doi.org/10.1109/lawp.2011.2165195

[8] S. Rodríguez Páez, A. Fajardo Jaimes, and C. I. Páez Rueda, Híbrido rat-race miniaturizado para la banda ISM 2, 4 GHZ, *Revista Tecnura*, **18** (2014), no. 38-52. https://doi.org/10.14483/udistrital.jour.tecnura.2014.4.a03

[9] J. M. Patin, N. R. Labadie and S. K. Sharma, Investigations on an H-fractal wideband microstrip filter with multi-passbands and a tuned notch band, *Prog. Electromagn. Res. B*, **22** (2010), 285–303. https://doi.org/10.2528/pierb10041001

[10] R. N. Baral and P. K. Singhal, Design of Microstrip Band Pass Fractal Filter for Suppression of Spurious Band, *Radioengineering*, **17** (2008), no. 4, 34-38.

[11] M. R. Da Silva, C. de L. Nóbrega, P. H. da F. Silva and A. G. D'Assunção, Dual-polarized band-stop FSS spatial filters using vicsek fractal geometry, *Microw. Opt. Technol. Lett.*, **55** (2013), no. 1, 31–34. https://doi.org/10.1002/mop.27242

[12] J. A. Fan, W.-H. Yeo, Y. Su, Y. Hattori, W. Lee, S.-Y. Jung, Y. Zhang, Z. Liu, H. Cheng, and L. Falgout, M. Bajema, T. Coleman, D. Gregoire, R. J. Larsen, Y. Huang and J. A. Rogers, Fractal design concepts for stretchable electronics, *Nat. Commun.*, **5** (2014). https://doi.org/10.1038/ncomms4266

[13] X.-J. Yang and D. Baleanu, Fractal heat conduction problem solved by local fractional variation iteration method, *Therm. Sci.*, **17** (2013), no. 2, 625–628. https://doi.org/10.2298/tsci121124216y

[14] Y. Chen and P. Cheng, Heat transfer and pressure drop in fractal tree-like microchannel nets, *Int. J. Heat Mass Transf.*, **45** (2002), no. 13, 2643–2648. https://doi.org/10.1016/s0017-9310(02)00013-3

[15] T. Ijiri, S. Owada, and T. Igarashi, The Sketch L-System: Global Control of Tree Modeling Using Free-Form Strokes, Chapter in *Smart Graphics*, Springer, 2006, 138–146. https://doi.org/10.1007/11795018_13

[16] P. Prusinkiewicz, Modeling plant growth and development, *Curr. Opin. Plant Biol.*, **7** (2004), no. 1, 79–83. https://doi.org/10.1016/j.pbi.2003.11.007

[17] C. Guoqing, Z. Yan, L. Hui and C. Weixing, Morphogenesis model-based virtual growth system for organs and plant of wheat, *Trans. Chinese Soc. Agric. Eng.*, **23** (2007), no. 3, 126-130.

[18] S. Kumar, C. Huang, G. Zheng, E. Bohm, A. Bhatele, J. C. Phillips, H. Yu, and L. V. Kale, Scalable molecular dynamics with NAMD on the IBM Blue Gene/L system, *IBM J. Res. Dev.*, **52** (2008), no. 1.2, 177–188. https://doi.org/10.1147/rd.521.0177

[19] P. Coates, T. Broughton and H. Jackson, *Exploring Three-Dimensional Design Worlds Using Lindenmayer Systems and Genetic Programming*, Evol. Des. by Comput., Morgan Kaufmann Publishers Inc., San Francisco, 1999.

[20] G. S. Hornby, H. Lipson and J. B. Pollack, Evolution of generative design systems for modular physical robots, *Proceedings 2001 ICRA. IEEE International Conference on Robotics and Automation*, Vol. 4, (2001), 4146–4151. https://doi.org/10.1109/robot.2001.933266

[21] F. Martínez, F. Martínez, and H. Montiel, Automatic design of heat sink using genetic algorithms, lindenmayer systems and digital image processing, *Eighth International Conference on Digital Image Processing (ICDIP 2016)*, (2016). https://doi.org/10.1117/12.2246540

Received: December 1, 2017; Published: December 19, 2017